

Cross-Polarization Optical Coherent Tomography in Comparative *in vivo* and *ex vivo* Studies of Optical Properties of Normal and Tumorous Brain Tissues

DOI: 10.17691/stm2017.9.4.22

Received September 4, 2017



E.B. Kiseleva, PhD, Researcher, Laboratory for Studies of Optical Structure of Biotissues, Research Institute of Biomedical Technologies¹;
K.S. Yashin, MD, Neurosurgeon²; Junior Researcher, Laboratory of High-Resolution Microscopy and Gene Technology, Research Institute of Biomedical Technologies¹;
A.A. Moiseev, PhD, Senior Researcher, Laboratory of High-Sensitivity Optical Measurements³;
M.A. Sirotkina, PhD, Senior Researcher, Laboratory for Individual Cancer Chemotherapy, Research Institute of Biomedical Technologies¹;
L.B. Timofeeva, PhD, Assistant Professor, Department of Histology with Cytology and Embryology¹;
V.V. Fedoseeva, Junior Researcher, Laboratory of Neuromorphology⁴;
A.I. Alekseeva, Junior Researcher, Laboratory of Neuromorphology⁴;
I.A. Medyanik, MD, DSc, Senior Researcher, Microneurosurgery Group²;
N.N. Karyakin, MD, DSc, Acting Rector¹;
L.Ya. Kravets, MD, DSc, Professor, Chief Researcher, Microneurosurgery Group²;
N.D. Gladkova, MD, DSc, Professor, Head of the Laboratory for Studies of Optical Structure of Biotissues, Research Institute of Biomedical Technologies¹

¹Nizhny Novgorod State Medical Academy, 10/1 Minin and Pozharsky Square, Nizhny Novgorod, 603005, Russian Federation;

²Privolzhsky Federal Medical Research Centre, Ministry of Health of the Russian Federation, 18 Verkhne-Volzhskaia naberezhnaya St., Nizhny Novgorod, 603155, Russian Federation;

³Institute of Applied Physics, Russian Academy of Sciences, 46 Ulyanova St., Nizhny Novgorod, 603155, Russian Federation;

⁴Research Institute of Human Morphology, 3 Tsurupy St., Moscow, 117418, Russian Federation

The aim of the study was to provide visual and quantitative evaluation of normal and tumorous brain tissue images obtained by cross-polarization optical coherence tomography (CP OCT) in comparative *in vivo* and *ex vivo* studies.

Materials and Methods. The study was conducted using CP OCT — a non-damaging optical method of tissue structure imaging, which is capable of obtaining real time 3D images 2.4×2.4×1.25 mm in size within a short time of 26 s. The object of the study were normal and tumorous brain tissues of 12 experimental rats of a Wistar line: 4 — intact, 4 — with an induced malignant 101.8-glioma model and 4 — with an induced malignant C6-glioma model. In the intact rats, the cortex and the white matter were studied, in the rats with tumors — the central part of the tumor on the cortical surface, first *in vivo* and then *ex vivo*. Quantitative data evaluation of the CP OCT images involved calculation of attenuation coefficients for each tissue type.

Results. A comparative qualitative image analysis of normal brain tissues and gliomas showed that the CP OCT images obtained *ex vivo* have the intensity and the attenuation rate (in both the initial and orthogonal polarizations) greater than those obtained *in vivo*. Quantitative analysis of the CP OCT images revealed significant statistical differences ($p < 0.02$) between the attenuation coefficients from both tumors and the white matter *in vivo* (5.5 [4.8; 5.8] mm⁻¹ for 101.8-glioma; 3.2 [2.4; 4.3] mm⁻¹ for C6-glioma; and 7.5 [7.0; 8.0] mm⁻¹ for the normal white matter) as compared with *ex vivo* (7.0 [5.9; 8.1] mm⁻¹ for 101.8-glioma; 6.8 [6.2; 7.9] mm⁻¹ for C6-glioma; and 9.0 [8.4; 9.5] mm⁻¹ for the normal white matter). For the cerebral cortex, no significant statistical difference was found (5.8 [4.9; 6.6] mm⁻¹ versus 6.3 [5.5; 7.1] mm⁻¹; $p = 0.34$). A comparison of the attenuation coefficients between the cortex and the white matter of the normal brain, as well as the white matter in the normal and malignant tissues, showed significant statistical differences both *in vivo* and *ex vivo*.

Conclusion. The results of a qualitative comparative analysis of optical properties of normal and tumorous brain tissues using CP OCT allow us to conclude that the images obtained *ex vivo* show a full qualitative similarity with the structures observed with the intravitreal CP OCT study. Quantitative evaluation of CP OCT signals demonstrated a significant difference in the attenuation coefficient ($p < 0.005$) between tumorous tissue, on the one hand, and normal white matter, on the other, both *ex vivo* and *in vivo*. However, when optical coefficients of tissues are evaluated *in vivo*, it is necessary to introduce adjustments based on the known differences between *ex vivo* and *in vivo* attenuation coefficients.

Key words: brain white matter; cortex; experimental tumor model; malignant glioma; cross-polarization optical coherence tomography; CP OCT; attenuation coefficient; *in vivo* and *ex vivo* studies..

For contacts: Elena B. Kiseleva, e-mail: kiseleva84@gmail.com

Presently, various intraoperative technologies (ultrasound, magnetic resonance imaging, fluorescence imaging) are commonly used in surgical treatment of gliomas; these techniques are aimed at improving safety and radicality of the tumor removal [1–4]. Recent studies demonstrated that the volume of tumor resection significantly correlates with life expectancy of patients in this group [5–8]. Therefore, a search for new technologies able to precisely differentiate between tumorous and non-tumorous brain tissue remains acute.

Optical bioimaging techniques are most promising in this regard [9], where optical coherence tomography (OCT) [10] and multiphoton microscopy/tomography [11] are capable of visualizing cyto- and myelo-architectonics of the brain.

Since the development of the OCT in 1991 and during the subsequent years of its continuous technological improvement, the method has become widespread in experimental medicine and in different clinical fields, including neurosurgery [12–15]. In current clinical practice, intraoperative OCT systems can be inbuilt in operating microscopes [15] and endoscopic instruments [16, 17]. However, the criteria for tumorous and non-tumorous brain tissue differentiation along the margin of tumor resection are still not fully developed. Several research groups have made significant contribution to the question of differentiation between an OCT signal from normal brain tissue and tumorous brain tissues in *in vivo* [18] and *ex vivo* [19] studies on experimental tumor models, on patients with gliomas *in vivo* [12, 20] and gliomas samples [12, 20, 21]. There are two approaches to the OCT data analysis: a qualitative analysis of OCT images [12, 21] and a quantitative analysis of the OCT signal with the calculation of various optical coefficients such as backscattering [21] and attenuation [12, 18, 22] coefficients.

Several OCT capabilities, such as performing real-time tissue microstructure analysis, not requiring a contrast agent injection, absence of damaging effect on the biotissue of its near-infrared radiation (700–1,300 nm), make it a promising intraoperative method of “optical biopsy”, which capable of distinguishing morphological characteristics of tissue.

The most reliable way of validating OCT results is a targeted histological examination of the tissue sample. However, for glial tumors, this way of validating the OCT method has some difficulties and limitations. When performed *in vivo* during surgery on a patient’s brain the measurements and their interpretation can be complicated by: 1) difficulties in obtaining a sharp OCT image due to oscillatory motion of the tissue due to pulse and respiratory cycle; 2) tissue deformation during its removal; 3) difficulties in access to the region of interest where the white matter is infiltrated by tumor; 4) active bleeding and use of hemostatic materials affecting the quality of OCT images [12]; 5) the time limit for the OCT study on the open brain, because a significant increase of the operating time is unacceptable.

Due to the above mentioned, researchers prefer to conduct *ex vivo* studies using a surgical biopsy material that contains only a glial tumor, white or gray matter, or both the tumor and non-tumorous brain tissue, as with this approach, it is easier to “target” the region of interest. An important advantage of *ex vivo* studies is the possibility of carrying out maximally targeted histological examinations to appropriately validate the optical method and its diagnostic accuracy. Its other advantage is the absence of strict time limitation, which makes it possible to perform multiple scans, monitor the image quality, and, if necessary, repeat the experiment to collect the required data. The results of visual evaluation and quantitative processing of *ex vivo* OCT images are free from inaccuracies caused by artifacts which are inevitable during *in vivo* studies.

Simultaneously, in *ex vivo* studies the loss of tissue perfusion and the change of sample volume due to distortion of the 3D tissue structure need to be accounted for in order to adequately interpret the OCT images and quantify the OCT signal. Animal studies show that the light attenuation profile at a resection edge within normal brain changes in a time-dependent manner, indicating that both exposure and tissue contusion alter the OCT signal [12]. Therefore, it is imperative to understand how the results obtained under *ex vivo* conditions will relate to those obtained during *in vivo* surgery because the OCT method is supposed to be ultimately used for intraoperative measurements. The possibility of using qualitative and quantitative evaluation criteria of the OCT images *ex vivo* for evaluating the OCT data obtained *in vivo* remains an open issue.

The method of cross-polarization OCT (CP OCT) is a version of polarization-sensitive OCT with certain advantages. Its main advantage is relative simplicity of analyzing the structure of CP OCT images. Its physical principle is the construction of two images: one based on the waves that save the initial polarization state after scattering, and the other containing waves that change to orthogonal polarization state. For the purpose of medical diagnostics, such analysis allows one to confirm the presence (or absence) of anisotropically scattering structures, such as collagen or myelin fibers, in the sample. By observing a change in the quantity and quality of anisotropic structures one can identify a pathological change in the given tissue. The CP OCT measurements are not sensitive to the orientation of the probe towards the anisotropic tissue structures but they are sensitive to cross-scattering and birefringence.

Interaction of polarized light with collagen as detected with CP OCT was utilized to identify vulnerable atherosclerotic plaques [23] and bladder carcinoma [24]. For the visualization of brain tissue and gliomas, the CP OCT was used in *in vivo* studies on the rat glioma model [25] and *ex vivo* studies on human gliomas of varying malignancy [26]. Those reports demonstrate a potential value of the CP OCT method in locating boundaries of tumor growth and determining the degree of malignancy.

The aim of the present study was to provide visual and quantitative evaluation of images obtained from normal and tumorous brain tissues using cross-polarization optical coherence tomography in comparative *in vivo* and *ex vivo* studies.

Materials and Methods

Tumor models. The study was carried out on 12 experimental animals (Wistar rats): 4 — intact, 4 — with transplantable malignant 101.8-glioma model and 4 — with transplantable malignant C6-glioma model. Both gliomas are chemically induced and were chosen as tumor models due to their similarity with human glioblastoma in terms of their morphological characteristics and a high degree of infiltration. The transplanted 101.8-glioma is a malignant glial tumor with high cellularity, numerous mitoses, and focal microvascular proliferation. It is characterized by extensive foci of necrosis and hemorrhage due to its rapid growth. In contrast, rat C6-glioma grows relatively slowly, therefore, large foci of hemorrhage and necrosis are not typical for this tumor; it is characterized by polymorphic — round or oval — cells and perivascular and perineuronal infiltration. In this study, optical properties of both tumors are studied because they have different growth rates and are morphologically heterogeneous.

The tumorous material was inoculated into rats at the Research Institute of Human Morphology of the Russian Academy of Sciences (Moscow) using the standard procedure [27]. During the tumor development and growth, the animals were kept under standard conditions. CP OCT studies were performed on the 10th–12th day after the transplantation of 101.8-glioma and on the 17th–19th day — for C6-glioma, when the tumors reached a visible size and spread through the cerebral cortex.

Our work with animals complied with the “Rules for the work using experimental animals” (Order of the Ministry of Health and Social Development of the Russian Federation dated August 23, 2010 No.708H “On the Approval of the Rules of Laboratory Practice”) and International Guiding Principles for Biomedical Research Involving Animals of 1985, while the ethical principles established by the European Convention for the Protection of Vertebrate Animals used for Experimental and Other Scientific Purposes (approved in Strasbourg on 18.03.1986 and confirmed in Strasbourg on 15.06.2006) were strictly observed. The experimental studies on animals were approved by the Ethics Committee of the Nizhny Novgorod State Medical Academy (Protocol 14 from 10 December 2013).

Cross-polarization optical coherent tomography device. The study was conducted using a high-speed multimodal optical coherent tomography device based on the spectral principle of signal reception. The device was developed at the Federal Research Center of the Institute of Applied Physics of the Russian Academy of Sciences (Nizhny Novgorod) [28, 29]. After scanning

the tissue, several images of its cross-section (from the surface into the depth) and images of the top view in real time were obtained. Polarized light was used as probing radiation, therefore, in addition to a standard structural OCT image (Figure 1, *columns 1 and 2, the upper parts of the images*), the second image complementary to the first one was created in the orthogonal polarization (Figure 1, *columns 1 and 2, the lower parts of the images*). With some technical modifications, the method is capable of producing angiographic images, which is important for *in vivo* studies [22].

A superluminescent diode is used as a radiation source with the following parameters: the central wavelength is 1,310 nm, the spectrum width ~100 nm, the power <5 mW; the depth resolution is 15 μ m, the transverse spatial resolution ~20 μ m. The speed of image acquisition is 20 kHz/s, and the time of recording of a 3D image (the planar dimensions and the height = 2.4×2.4×1.25 mm) is 26 s. From the obtained 3D arrays of OCT data (one 3D array contains 256 B-scans in each polarization mode and 65536 A-scans), B-scans typical for the specific tissue were selected for further analysis and presentation. The scans are stored as 2D images with sizes of 2.4 mm (width) × 1.25 mm (height) in the co- and cross-polarization modes.

The CP OCT device is equipped with an end-type fiber optic probe with an external diameter of 8 mm, which is brought close to the tissue surface without touching it.

Design of the CP OCT studies *in vivo* and *ex vivo*.

The CP OCT studies on tumorous and normal brain tissues *in vivo* were conducted after craniotomization. All the surgical interventions were performed using a stereotaxic device equipped with a stereomicroscope Leica M60 (Leica Microsystems, Germany, objective ×1, eyepieces ×10). During the CP OCT study, the animals were kept under anesthesia (Zoletil 50 and 2% Romethar).

CP OCT images of the normal cortex (left hemisphere) and the normal white matter (right hemisphere) were obtained from the parietal area of the brain at the distance of 2–5 mm from the central gyrus; CP OCT images of 101.8 and C6 gliomas were obtained from the central region of the tumor visible on the cortical surface. In total 4 intact and 8 tumor-bearing rats (4 rats for each model) were used in the study. Prior to the measurements on the white matter *in vivo*, the cortex had been cleaned layer by layer. The scan time of one area of interest did not exceed 5 min. After that, the borders of the scanned area were marked with histological ink, and the animals were withdrawn from the experiment. The brain was removed and placed under the OCT probe to acquire images from the respective areas of the cerebral cortex, the white matter or the tumor.

16 areas of interest were scanned *in vivo* and as many *ex vivo*; 16 samples were taken for histological examination. A total of 98 arrays of OCT data were obtained and analyzed; each area of interest was

scanned to get and store two or three 3D OCT images. For the quantitative analysis, 92 images were selected (see the Table).

Quantitative processing of the CP OCT data.

The data from the 3D images were processed with Anaconda 4.3.1 (Python v. 3.6) software. For each A-scan representing the depth-dependent attenuation profile of the OCT signal, the attenuation coefficient of the initial radiation in the given sample was calculated [18]; then the entire data volume was averaged. To take into account the polarization effects, the attenuation coefficient was calculated from the Pythagorean sum of the signals in the initial and orthogonal polarizations [23]. The signals recorded through the co- and cross channels were squared, added and turned logarithmic. The resulting curves were presented as linear functions; the attenuation coefficient was defined as the first power coefficient in the obtained equation. For a better fit of the experimental data to the selected model, the calculations were limited to a reduced depth range: 100–300 μm from the image surface.

The attenuation coefficients were calculated for 4 groups of tissues: cerebral cortex, white matter, 101.8-glioma, and C6-glioma. The attenuation coefficients found *in vivo* and *ex vivo* were compared within each group; the significance of the differences between the normal tissue and the tumor was tested for the values of attenuation coefficients *in vivo* and *ex vivo*.

Histological examination. To verify the structure of normal and tumorous brain tissue from the areas of the CP OCT measurements, the samples were histologically analyzed. The tissue samples were fixed in a 10% solution of buffered formalin for 48 h. After a series of washes, the material was embedded into paraffin at 57°C. Then the sections were stained with hematoxylin and eosin. The histological slides were viewed and characterized by a morphologist and photographed under a transmission Leica DM2500 DFC (Leica Microsystems, Germany) microscope equipped with a digital camera.

Statistical processing of the results was carried out using statistical analysis package Statistica 10.0. For calculating the attenuation coefficient from the 3D CP OCT images, the mean value of all A-scans was derived; for each experimental group the attenuation coefficient was expressed as Me [Q1; Q3]. To test the statistical hypotheses, nonparametric methods were used. To compare the quantitative data of two independent groups, the Mann-Whitney U test was used.

Results and Discussion

A comparative analysis of CP OCT images of normal brain tissues and gliomas obtained *in vivo* and *ex vivo* — a qualitative assessment. A visual assessment of CP OCT images makes it possible to identify differences between signals from the cortex, the white matter, and the tumour. In Figure 1, typical CP OCT images of the normal cortex, the white matter and 101.8 and C6 gliomas *in vivo* (a1)–(d1) and *ex vivo*

(a2)–(d2) along with the corresponding histology of the imaged tissues (a3)–(d3) are shown.

The CP OCT signals obtained *ex vivo* is more intensive and have greater attenuation rate (in both the initial and orthogonal polarizations) than those obtained *in vivo*. Notably, there are also structural differences between the *ex vivo* and *in vivo* images of the cerebral cortex. In the *in vivo* studies, CP OCT images show a specific vertical striation arising from “shadows” of the blood vessels located just under the tissue surface (see Figure 1 (a1)); this striation is practically not visible on the *ex vivo* images due to vasoconstriction (Figure 1 (a2)). For the CP OCT images of the white matter and both experimental tumors, no significant differences in the signal features between the *ex vivo* and *in vivo* experiments were detected (Figure 1 (b1)–(d2)).

White matter and the tumorous tissue can be differentiated by visual differences of its CP OCT signals, as reported earlier [25]. The normal white matter produces (in both polarizations) a uniform high-amplitude signal in the form of a narrow band (Figure 1 (b1), (b2)). The white matter consists of densely packed myelinic nerve fibers (Figure 1 (b3)) that effectively dissipate the probing radiation both in the initial and in the orthogonal polarization.

Tumorous tissue consists of randomly located irregular cells of various shapes and sizes, a large number of vessels (Figure 1 (d3)), as well as foci of large and small hemorrhages and necrosis, especially in 101.8-glioma (Figure 1 (c3), (d3)). These morphological features of the tumorous tissue determine the heterogeneity of the OCT signal in both polarization states (Figure 1 (c1), (c2)), although this heterogeneity is more contrasted in the orthogonal polarization. The degree of light backscattering from the tumor cell membranes is much lower than that from the myelin sheath of a nerve fiber (that contains numerous membranes); therefore, the total intensity of the OCT signal from tumors (Figure 1 (c1) (c2), (d1), (d2)) is significantly lower than that in the white matter of the brain (Figure 1 (b1), (b2)). At the same time, the CP OCT image can be quite homogeneous (Figure 1 (d1), (d2)) if the given tumor focus contains no necrosis or hemorrhages, as shown, for example, in the case of C6-glioma (Figure 1 (d3)). The attenuation rate of the OCT signal in this case is low. Areas of hemorrhages and necrosis have strong scattering properties and are therefore represented on CP OCT images by areas with high signal amplitudes. In its entirety, the signal from a tumorous tissue is markedly heterogeneous as shown in the example of 101.8-glioma (Figure 1 (c1), (c2)).

Comparative analysis of CP OCT images of normal brain tissues and gliomas obtained *in vivo* and *ex vivo* — a quantitative assessment.

A quantitative analysis of the CP OCT data revealed statistically significant differences in the attenuation coefficients of the normal white matter and experimental gliomas between the *in vivo* and *ex vivo* measurements

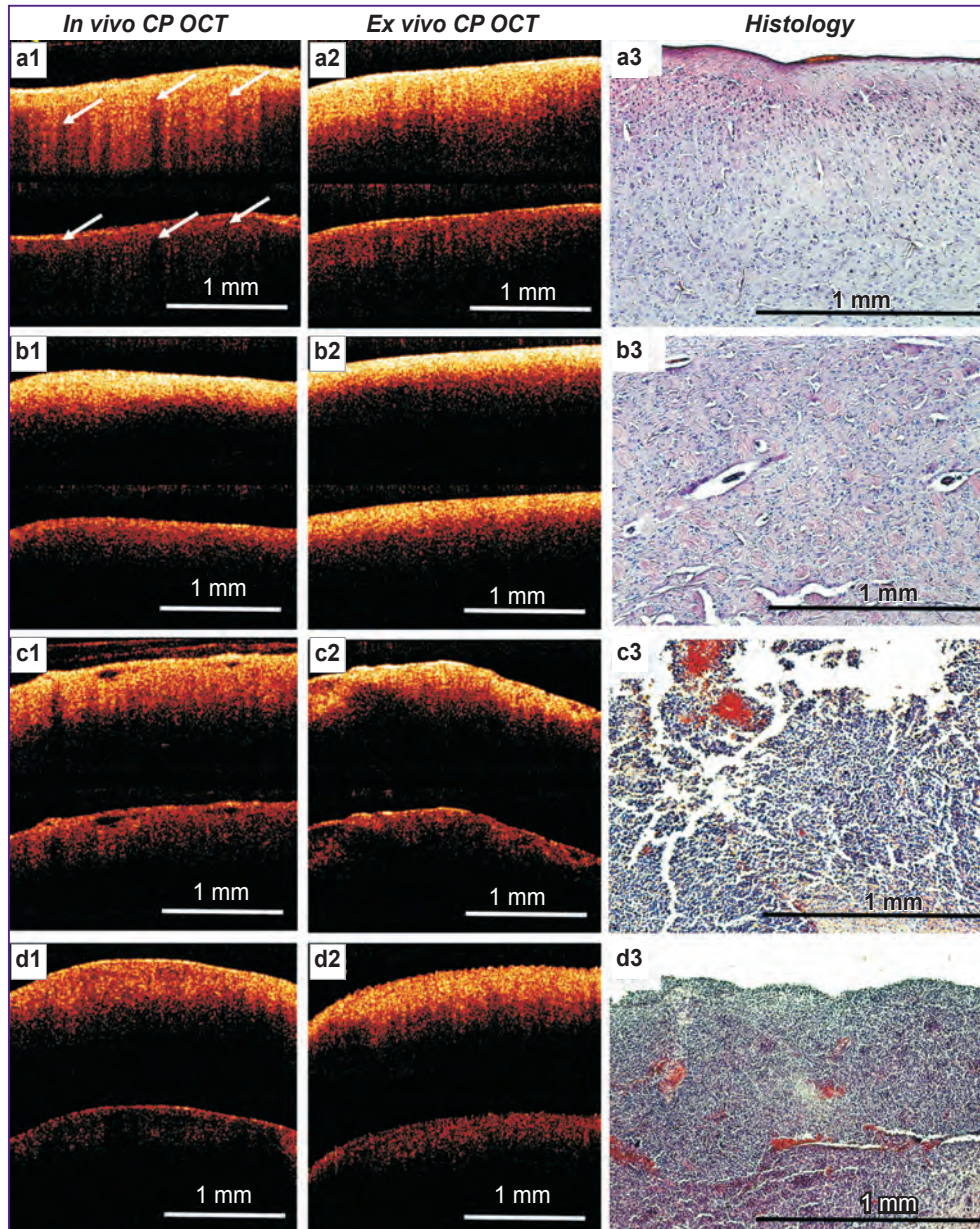


Figure 1. CP OCT images obtained from *in vivo* (a1)–(d1) and *ex vivo* (a2)–(d2) studies and the corresponding histology (a3)–(d3):

(a1), (a2) cortex of a normal brain; (b1), (b2) white matter of the normal brain; (c1), (c2) 101.8-glioma; (d1), (d2) C6-glioma; the CP OCT images are shown in two polarizations: the upper part shows the signal in the initial (co-) polarization, the lower part — in the orthogonal (cross-) polarization; the white arrows indicate “shadows” from blood vessels (a1); the OCT signal is shown in the logarithmic scale

(see the Table, Figure 2 (b)–(d)). The values of attenuation coefficients in the white matter and 101.8 and C6 gliomas in the *ex vivo* studies were higher than those found *in vivo*, which is due to tissue solidification caused by dehydration [30]. Importantly, according to the visual assessment, there was also a slight increase in the CP OCT signal intensity *ex vivo* in comparison with the signals obtained *in vivo* (Figure 1 (a1), (a2), (b1), (b2), (c1), (c2), (d1), (d2)).

For the cerebral cortex, according to the quantitative

evaluation of CP OCT images, there was a similar trend toward an increase in the attenuation coefficient found *ex vivo* ($6.3 [5.5; 7.1] \text{ mm}^{-1}$) as compared with that *in vivo* ($5.8 [4.9; 6.6] \text{ mm}^{-1}$); however, the difference was not statistically significant ($p=0.34$) (see the Table, Figure 2 (a)). A possible explanation of this trend is that the attenuation coefficient calculated from the *in vivo* CP OCT images may be over-evaluated due to the presence in the cortex of numerous blood vessels where the OCT signal attenuates faster than in the myelinated structures

The attenuation coefficients obtained in the quantitative analysis of three-dimensional CP OCT data of normal brain tissues and malignant gliomas *in vivo* and *ex vivo* (Me [Q1; Q3])

| Tissue type | Attenuation coefficient (mm ⁻¹) | | Attenuation coefficient ratio <i>ex vivo</i> / <i>in vivo</i> | p (<i>ex vivo</i> – <i>in vivo</i>) |
|-------------------------------|---|-----------------------|---|---------------------------------------|
| | <i>in vivo</i> | <i>ex vivo</i> | | |
| Brain cortex | 5.8 [4.9; 6.6] (n=11) | 6.3 [5.5; 7.1] (n=17) | 1.08 | 0.34 |
| White matter | 7.5 [7.0; 8.0] (n=12) | 9.0 [8.4; 9.5] (n=15) | 1.20 | 0.0008 |
| 101.8-glioma | 5.5 [4.8; 5.8] (n=8) | 7.0 [5.9; 8.1] (n=12) | 1.27 | 0.007 |
| C6-glioma | 3.2 [2.4; 4.3] (n=8) | 6.8 [6.2; 7.9] (n=9) | 2.10 | 0.016 |
| p (white matter–101.8-glioma) | 0.0004 | 0.0001 | | |
| p (white matter–C6-glioma) | 0.004 | 0.0004 | | |
| p (white matter–cortex) | 0.0002 | 0.000007 | | |
| p (cortex–101.8-glioma) | 0.36 | 0.11 | | |
| p (cortex–C6-glioma) | 0.01 | 0.51 | | |

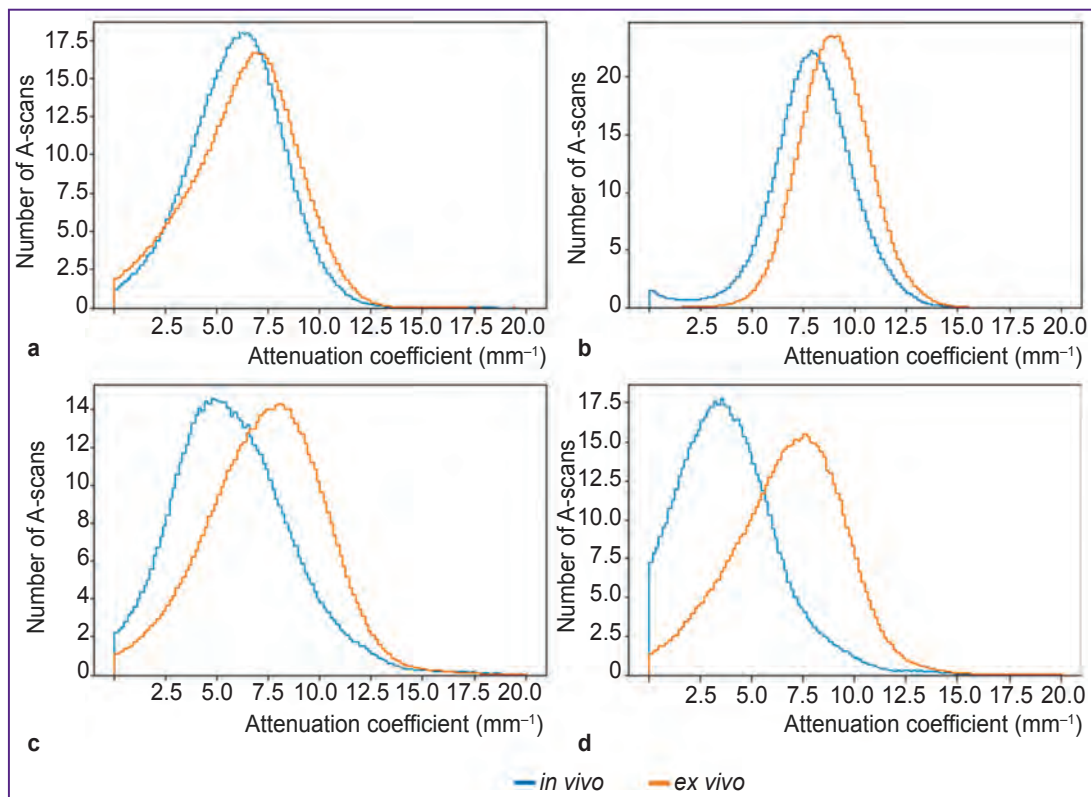


Figure 2. Histograms of the attenuation coefficient data for *in vivo* and *ex vivo* studies on different tissues: (a) normal cerebral cortex; (b) normal white matter; (c) experimental 101.8-glioma; (d) experimental C6-glioma

of the brain cortex. To obtain a more reliable comparison between the *in vivo* and *ex vivo* results, it is necessary to adjust the algorithm for calculating the attenuation

coefficient for CP OCT images obtained *in vivo*, taking into account the presence of blood vessels.

A comparison of the attenuation coefficients of signals

from the normal cortex and the white matter, as well as from normal brain tissue and malignant gliomas showed the following. The differences between the attenuation coefficient values from both tumors and the white matter, in both *in vivo* (see the Table, Figure 3 (c)) and *ex vivo* analysis (see the Table, Figure 3 (d)), were found to be statistically significant. This is consistent with the results of the visual assessment of typical OCT images of the experimental tumors and the white matter, where the white matter is represented by a narrow band of high intensity signal and is characterized by a rapid signal

decrease, while the tumor is characterized by a less intense inhomogeneous signal with a slow attenuation.

The attenuation coefficient of the OCT signal from the cerebral cortex is statistically significantly lower than that of the signal from the white matter when tested *in vivo* (see the Table, Figure 3 (a)) and *ex vivo* (see the Table, Figure 3 (b)); however, it is comparable with the values of the coefficients from the experimental tumors (see the Table, Figure 3 (e), (f)).

The exception in our study were the *in vivo* values of the attenuation coefficient of the signal from C6-glioma,

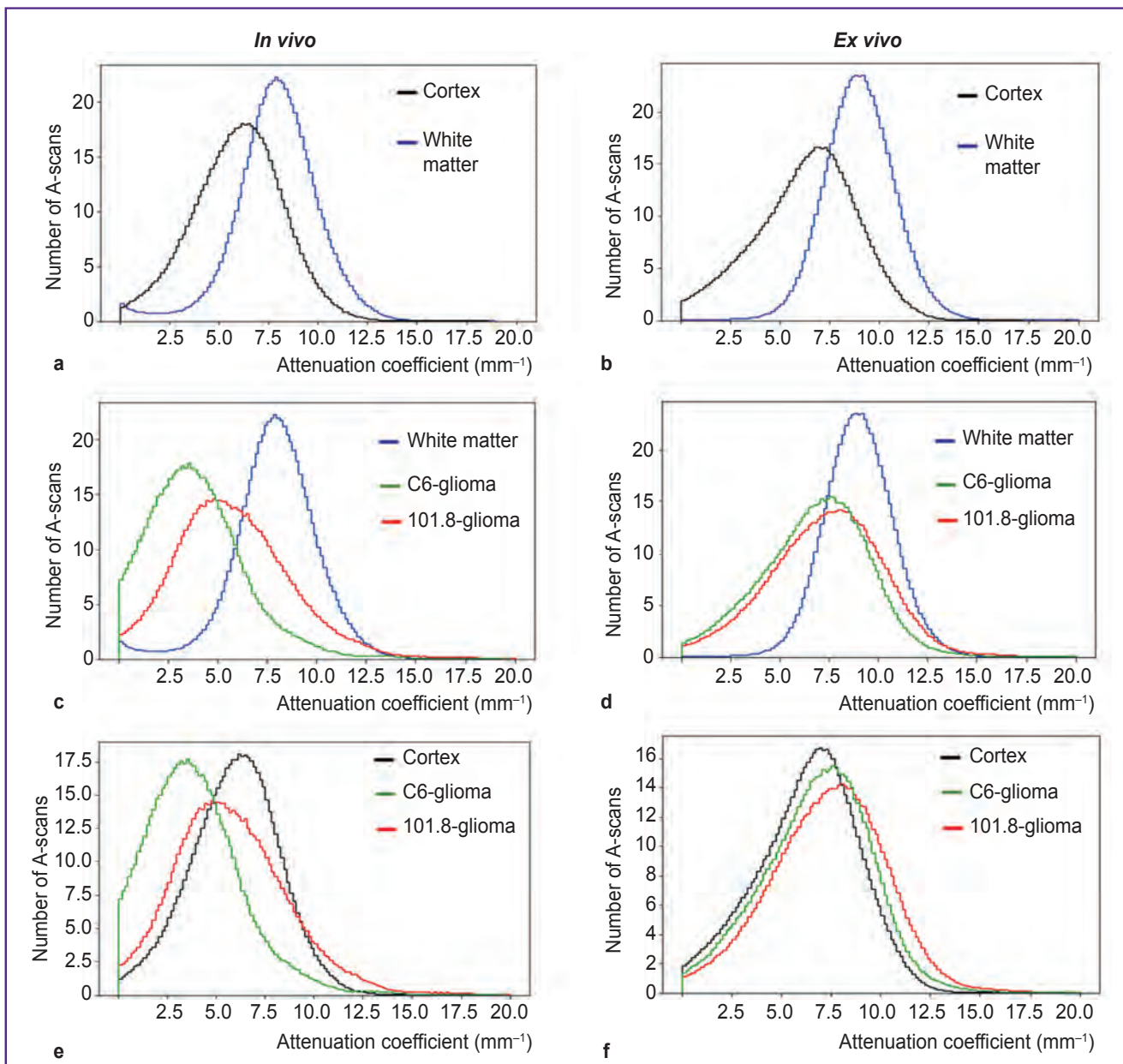


Figure 3. Histograms of the attenuation coefficient data for *in vivo* (a), (c), (e) and *ex vivo* (b), (d), (f) comparative studies on different tissues:

(a), (b) normal white matter and normal cortex; (c), (d) normal white matter and 101.8 and C6 gliomas; (e), (f) normal cortex and 101.8 and C6 gliomas

which were statistically significantly lower than the values of the signal from the cortex (3.2 [2.4; 4.3] vs 5.8 [4.9; 6.6] mm^{-1} , $p=0.01$). At the same time, the attenuation coefficient of the OCT signal from 101.8-glioma in the *in vivo* study was comparable to the attenuation coefficient in the cerebral cortex (5.5 [4.8; 5.8] vs 5.8 [4.9; 6.6] mm^{-1} , $p=0.36$), which might be due to numerous hemorrhages and necrotic foci in this model. In the *ex vivo* study, the differences become less pronounced due to an increase in the attenuation coefficient of the OCT signal from the cerebral cortex.

The results of this study showed that optical properties of tumorous and normal brain tissues vary depending on the conditions of their study. The values of the attenuation coefficients in normal tissues and tumors *ex vivo* are higher than those *in vivo*; for the white matter and the tumors, these differences reach statistical significance. Notably, consistently higher values of the attenuation coefficient in the white matter as compared with those in the tumors are found in both *in vivo* and *ex vivo* studies; for the cerebral cortex this consistency does not hold true. Therefore, we believe that the results obtained *ex vivo* require adjustment before being extrapolated to the *in vivo* conditions.

The results obtained *ex vivo* show statistically significant differences in the attenuation coefficients between the white matter and the malignant tumors (9.0 [8.4; 9.5] mm^{-1} for the white matter vs 7.0 [5.9; 8.1] mm^{-1} for 101.8-glioma, $p=0.001$ and vs 6.8 [6.2; 7.9] mm^{-1} for C6-glioma, $p=0.001$). These results are in good agreement with the results of [18], where the authors used postoperative tissue samples to show that the attenuation coefficient in the white matter ($6.2 \pm 0.8 \text{ mm}^{-1}$) was significantly higher ($p=0.002$) compared to that of the tissue excised from the center of a highly malignant tumor ($3.9 \pm 1.6 \text{ mm}^{-1}$). The higher attenuation coefficients obtained in our study may be explained by the calculation method. In [18], the attenuation coefficients were calculated for certain regions of interest on the OCT image using algorithms for signal averaging. In our study the method of coefficients calculating was simplified: all A-scans of 3D image were processed, no special algorithms to prepare the images were used, and a fixed range of depths was set.

Conclusion. In conclusion, the comparative qualitative and quantitative analysis of the optical properties of normal and tumorous brain tissues, studied with CP OCT, shows that:

for *in vivo* differentiation of tumorous — non-tumorous brain tissues using the optical coefficients obtained *ex vivo*, the values should be recalculated considering the known *ex vivo/in vivo* ratios specific for the tissue type;

due to the differences in the OCT signals and the values of attenuation coefficients between the malignant gliomas and the white matter of the brain, as well as between the white matter and the cortex, in both *in vivo* and *ex vivo* studies, the results of the visual and quantitative evaluation of CP OCT data obtained *ex vivo*,

can be used with some degree of certainty to interpret the *in vivo* signal. The exception is the cerebral cortex where the structural features observed *in vivo* are not typical for most tissues; this peculiarity makes it possible to distinguish the cortex by visually assessing a CP OCT image.

Financial Support. The experiments, quantitative processing and statistical analysis were funded by a grant from the Russian Science Foundation, contract No.16-15-10391; the development of the method for calculating the optical coefficients was supported by the Russian Foundation for Basic Research, contract No.16-32-60178 mole_a_dk.

Conflict of Interest. The authors have no conflict of interest.

References

- Potapov A.A., Goryaynov S.A., Okhlopov V.A., Pitskhelauri D.I., Kobayakov G.L., Zhukov V.Y., Gol'bin D.A., Svistov D.V., Martynov B.V., Krivoschapkin A.L., Gaytan A.S., Anokhina Y.E., Varyukhina M.D., Gol'dberg M.F., Kondrashov A.V., Chumakova A.P. Clinical guidelines for the use of intraoperative fluorescence diagnosis in brain tumor surgery. *Zh Vopr Neurokhir Im N N Burdenko* 2015; 79(5): 91–101, <https://doi.org/10.17116/neiro201579591-101>.
- Selbekk T., Jakola A.S., Solheim O., Johansen T.F., Lindseth F., Reinertsen I., Unsgard G. Ultrasound imaging in neurosurgery: approaches to minimize surgically induced image artefacts for improved resection control. *Acta Neurochir (Wien)* 2013; 155(6): 973–980, <https://doi.org/10.1007/s00701-013-1647-7>.
- Semin P.A., Krivoschapkin A.L., Melidi E.G., Kanygin V.V. Frameless neuronavigation and its application in the course of surgery of cerebral mass lesions. *Neyrokhirurgiya* 2004; 2: 20–24.
- Fahlbusch R., Samii A. Editorial: Intraoperative MRI. *Neurosurg Focus* 2016; 40(3): E3, <https://doi.org/10.3171/2015.12.focus15631>.
- Almeida J.P., Chaichana K.L., Rincon-Torroella J., Quinones-Hinojosa A. The value of extent of resection of glioblastomas: clinical evidence and current approach. *Curr Neurol Neurosci Rep* 2014; 15(2): 517, <https://doi.org/10.1007/s11910-014-0517-x>.
- Díez Valle R., Tejada Solís S., Idoate Gastearena M.A., García de Eulate R., Domínguez Echávarri P., Aristu Mendiroz J. Surgery guided by 5-aminolevulinic fluorescence in glioblastoma: volumetric analysis of extent of resection in single-center experience. *J Neurooncol* 2011; 102(1): 105–113, <https://doi.org/10.1007/s11060-010-0296-4>.
- Sanai N., Berger M.S. Extent of resection influences outcomes for patients with gliomas. *Rev Neurol (Paris)* 2011; 167(10): 648–654, <https://doi.org/10.1016/j.neurol.2011.07.004>.
- Stummer W., Pichlmeier U., Meinel T., Wiestler O.D., Zanella F., Reulen H.J. Fluorescence-guided surgery with 5-aminolevulinic acid for resection of malignant glioma: a randomised controlled multicentre phase III trial. *Lancet Oncol* 2006; 7(5): 392–401, [https://doi.org/10.1016/s1470-2045\(06\)70665-9](https://doi.org/10.1016/s1470-2045(06)70665-9).
- Vasefi F., MacKinnon N., Farkas D.L., Kateb B. Review of the potential of optical technologies for cancer diagnosis in

neurosurgery: a step toward intraoperative neurophotonics. *Neurophotonics* 2016; 4(1): 011010, <https://doi.org/10.1117/1.nph.4.1.011010>.

10. Yashin K.S., Kravets L.Y., Gladkova N.D., Gelikonov G.V., Medyanik I.A., Karabut M.M., Kiseleva E.B., Shilyagin P.A. Optical coherence tomography in neurosurgery. *Zh Vopr Neurokhir Im N N Burdenko* 2017; 81(3): 107–115, <https://doi.org/10.17116/neiro2017813107-115>.

11. Kantelhardt S.R., Kalasauskas D., König K., Kim E., Weinigel M., Uchugonova A., Giese A. In vivo multiphoton tomography and fluorescence lifetime imaging of human brain tumor tissue. *J Neurooncol* 2016; 127(3): 473–482, <https://doi.org/10.1007/s11060-016-2062-8>.

12. Böhringer H.J., Lankenau E., Stellmacher F., Reusche E., Hüttmann G., Giese A. Imaging of human brain tumor tissue by near-infrared laser coherence tomography. *Acta Neurochir (Wien)* 2009; 151(5): 507–517, <https://doi.org/10.1007/s00701-009-0248-y>.

13. Herrero-Garibi J., Cruz-Gonzalez I., Parejo-Diaz P., Jang I.K. Optical coherence tomography: its value in intravascular diagnosis today. *Rev Esp Cardiol* 2010; 63(8): 951–962, [https://doi.org/10.1016/s1885-5857\(10\)70189-4](https://doi.org/10.1016/s1885-5857(10)70189-4).

14. Mathews M.S., Su J., Heidari E., Levy E.I., Linskey M.E., Chen Z. Neuroendovascular optical coherence tomography imaging and histological analysis. *Neurosurgery* 2011; 69(2): 430–439, <https://doi.org/10.1227/neu.0b013e318212bc4>.

15. Lankenau E.M., Krug M., Oelckers S., Schrage N., Just T., Hüttmann G. iOCT with surgical microscopes: a new imaging during microsurgery. *Advanced Optical Technologies* 2013; 2(3), <https://doi.org/10.1515/aot-2013-0011>.

16. Zagaynova E., Gladkova N., Shakhova N., Gelikonov G., Gelikonov V. Endoscopic OCT with forward-looking probe: clinical studies in urology and gastroenterology. *J Biophotonics* 2008; 1(2): 114–128, <https://doi.org/10.1002/jbo.200710017>.

17. Sun C., Lee K.K., Vuong B., Cusimano M.D., Brukson A., Mauro A., Munce N., Courtney B.K., Standish B.A., Yang V.X. Intraoperative handheld optical coherence tomography forward-viewing probe: physical performance and preliminary animal imaging. *Biomed Opt Express* 2012; 3(6): 1404–1412, <https://doi.org/10.1364/boe.3.001404>.

18. Kut C., Chaichana K.L., Xi J., Raza S.M., Ye X., McVeigh E.R., Rodriguez F.J., Quinones-Hinojosa A., Li X. Detection of human brain cancer infiltration ex vivo and in vivo using quantitative optical coherence tomography. *Sci Transl Med* 2015; 7(292): 292ra100, <https://doi.org/10.1126/scitranslmed.3010611>.

19. Böhringer H.J., Boller D., Leppert J., Knopp U., Lankenau E., Reusche E., Hüttmann G., Giese A. Time-domain and spectral-domain optical coherence tomography in the analysis of brain tumor tissue. *Lasers Surg Med* 2006; 38(6): 588–597, <https://doi.org/10.1002/lsm.20353>.

20. Bizheva K., Unterhuber A., Hermann B., Povazay B., Sattmann H., Fercher A.F., Drexler W., Preusser M., Budka H., Stingl A., Le T. Imaging ex vivo healthy and pathological human brain tissue with ultra-high-resolution optical coherence

tomography. *J Biomed Opt* 2005; 10(1): 11006, <https://doi.org/10.1117/1.1851513>.

21. Boppart S.A., Brezinski M.E., Pitris C., Fujimoto J.G. Optical coherence tomography for neurosurgical imaging of human intracortical melanoma. *Neurosurgery* 1998; 43(4): 834–841, <https://doi.org/10.1097/00006123-199810000-00068>.

22. Yuan W., Kut C., Liang W., Li X. Robust and fast characterization of OCT-based optical attenuation using a novel frequency-domain algorithm for brain cancer detection. *Sci Rep* 2017; 7: 44909, <https://doi.org/10.1038/srep44909>.

23. Gubarkova E.V., Kirillin M.Y., Dudenkova V.V., Timashev P.S., Kotova S.L., Kiseleva E.B., Timofeeva L.B., Belkova G.V., Solovieva A.B., Moiseev A.A., Gelikonov G.V., Fiks I.I., Feldchtein F.I., Gladkova N.D. Quantitative evaluation of atherosclerotic plaques using cross-polarization optical coherence tomography, nonlinear, and atomic force microscopy. *J Biomed Opt* 2016; 21(12): 126010, <https://doi.org/10.1117/1.jbo.21.12.126010>.

24. Kiseleva E., Kirillin M., Feldchtein F., Vitkin A., Sergeeva E., Zagaynova E., Streltsova O., Shakhov B., Gubarkova E., Gladkova N. Differential diagnosis of human bladder mucosa pathologies in vivo with cross-polarization optical coherence tomography. *Biomed Opt Express* 2015; 6(4): 1464–1476, <https://doi.org/10.1364/boe.6.001464>.

25. Yashin K.S., Karabut M.M., Fedoseeva V.V., Khalansky A.S., Matveev L.A., Elagin V.V., Kuznetsov S.S., Kiseleva E.B., Kravets L.Y., Medyanik I.A., Gladkova N.D. Multimodal optical coherence tomography in visualization of brain tissue structure at glioblastoma (experimental study). *Sovremennye tehnologii v medicine* 2016; 8(1): 73–81, <https://doi.org/10.17691/stm2016.8.1.10>.

26. Yashin K.S., Gubarkova E., Kiseleva E., Kuznetsov S.S., Karabut M.M., Medyanik I.A., Kravets L.Y., Gladkova N.D. Ex vivo imaging of human gliomas by cross-polarization optical coherence tomography: pilot study. *Sovremennye tehnologii v medicine* 2016; 8(3): 14–22, <https://doi.org/10.17691/stm2016.8.4.02>.

27. Khalansky A.S., Kondakova L.I., Gelperina S.E. Transplanted rat glioma 101.8. II. The application in experimental neurooncology and therapy. *Klinicheskaya i eksperimental'naya morfologiya* 2014; 1(9): 50–59.

28. Gelikonov V.M., Gelikonov G.V. New approach to cross-polarized optical coherence tomography based on orthogonal arbitrarily polarized modes. *Laser Physics Letters* 2006; 3(9): 445–451, <https://doi.org/10.1002/lapl.200610030>.

29. Matveev L.A., Zaitsev V.Y., Gelikonov G.V., Matveyev A.L., Moiseev A.A., Ksenofontov S.Y., Gelikonov V.M., Sirotkina M.A., Gladkova N.D., Demidov V., Vitkin A. Hybrid M-mode-like OCT imaging of three-dimensional microvasculature in vivo using reference-free processing of complex valued B-scans. *Opt Lett* 2015; 40(7): 1472–1475, <https://doi.org/10.1364/ol.40.001472>.

30. Rodriguez C.L., Szu J.I., Eberle M.M., Wang Y., Hsu M.S., Binder D.K., Park B.H. Decreased light attenuation in cerebral cortex during cerebral edema detected using optical coherence tomography. *Neurophotonics* 2014; 1(2): 025004, <https://doi.org/10.1117/1.nph.1.2.025004>.